

Oil sorbers based on renewable sources and coffee grounds

Fernanda D. Marques,¹ Fernando G. Souza Jr.,^{1,2} Geiza E. Oliveira^{1,3}

¹Laboratório De Biopolímeros E Sensores - Instituto De Macromoléculas, Universidade Federal Do Rio De Janeiro, Brasil

²Programa De Engenharia Civil, COPPE, Centro De Tecnologia - Cidade, Universitária, Av. Horácio Macedo, 2030, Bloco B. Universidade Federal, De Rio De Janeiro, Brasil

³Departamento De Química - Centro De Ciências Exatas, Universidade Federal Do Espírito Santo, Brasil

Correspondence to: G. E. Oliveira (E-mail: geizaesperandio@gmail.com)

ABSTRACT: This work presents useful composites for oil spill cleanup processes. These systems are composed of a polyester matrix loaded with coffee ground powder and maghemite. They were prepared by *in situ* polymerization. The aliphatic monomers proportion—castor oil and glycerin—was studied with the aim of understanding the effect of feed ratio on the product properties. The materials were studied using several techniques, including Fourier Transform Infrared Spectroscopy, Ultraviolet-visible Spectrophotometry, and Wide Angle X-ray Scattering, with magnetic force tests used for the characterization of materials. Density tests showed the presence of coffee grounds causes an important reduction in the density values of composites, improving their flotation. The interaction between composites and petroleum is more than twice that between composites and water. Moreover, for all magnetizable composites, the removal capability was (25.1 ± 1.2) g/g (petroleum/composite), allowing us to state that this is a promising material for use in oil spill cleanup processes. © 2015 Wiley Periodicals, Inc. *J. Appl. Polym. Sci.* **2016**, *133*, 43127.

KEYWORDS: composites; magnetism and magnetic properties; nanoparticles; nanowires and nanocrystals; oil & gas

Received 7 May 2015; accepted 31 October 2015

DOI: 10.1002/app.43127

INTRODUCTION

Crude oil spill accidents are among the worst environmental catastrophes. The increasing consumption has caused a growth in the production, transport, and storage steps. These steps present risks related to environmental oil spills. The damages caused in this kind of accident are, most of the times, irreversible, which shows the importance of researching cleanup methods.¹

Crude oil absorbers are materials that are able to clean and remove oily compounds from the water surface. Currently, several studies are being conducted aimed at this kind of application.^{2–8} This type of material can be considered a beneficial alternative because they may significantly reduce the impact of this kind of accident. The main natural absorbers are leaves from different plants,⁹ chitin, chitosan and their derivatives.¹⁰ Among the synthetic absorbers, polymeric resins from renewable sources are highlighted.^{11,12}

Alkyd resins are very much used in the paint industry based on several formulations.¹³ However, these polyesters, when prepared as a thermoset, can be used as good crude oil absorbers. These kinds of material are formed basically to aliphatic and/or aromatic chains which increases their lipophilicity, closely resembling that of crude oil.^{14,15}

Coffee is consumed around the world, thus producing lots of coffee grounds. Annually, more than 7.4 million tons of coffee grounds are discarded; this can have a significant environmental impact, depending on the discard conditions.¹⁶ Coffee grounds have a low density and a chemical composition that is similar to several organic compounds, including crude oil. These features of coffee grounds can be used to prepare an absorber for the oil spill cleanup process, which can accelerate the crude oil removal process or promote improved properties in the materials.

Magnetizable materials are those that answer to an applied magnetic field. Normally, this kind of material is composed of several domains, distributed randomly, which provides a zero net magnetic moment. However, magnetizable nanoparticles present single domain, a monodomain, inside each particle, because of their nanometric scale. This feature allows the magnetizable nanoparticles show superparamagnetic behavior, which means, there is no residual magnetization after the magnetic field removal.¹⁷ Besides vegetable fillers, the addition of magnetizable nanoparticles allows the production of materials that are able to catch and remove crude oil from water using a magnetic field by an on/off behavior.¹⁴ This kind of behavior makes possible to use the electromagnet to remove the material from water after crude oil absorption.

The main aim of this study was to develop and understand new multiphase systems containing magnetic properties, able to present an on/off magnetic behavior and to remove crude oil from water surface. The materials obtained were evaluated using several analytical techniques, including Fourier transform infrared spectroscopy (FTIR), X ray diffraction (XRD), thermogravimetric analysis (TGA), cross-link degree, magnetic strength, and crude oil removal capability. Among the main results, FTIR confirmed the polymeric resin synthesis, and evidence was provided that the particles are dispersed in the polymeric matrix. The XRD results enabled calculation of the size of magnetizable particles inside the materials, which confirmed that the particles were not altered during the mixture process. In turn, density tests demonstrated the materials' flotation capability, as expected, while the cross-link degree determination permitted information about the resin structure to be obtained. The resin was found to be insoluble and infusible, making it perfect for use as a crude oil absorber, and it was also possible for the absorber material to be recycled and recovered after the removal of oil. In addition, the developed absorber presents a crude oil removal capability of more than 25 crude oil parts for composite part. This is one of the best results obtained by this research group.^{2-4,14} Therefore, this work can be considered a step forward in this subject, and presents novel uses for byproducts, such as glycerin, and wastes, such as coffee grounds, which creates added value.

EXPERIMENTAL

Materials: Hexahydrated iron chloride ($\text{FeCl}_3 \cdot 6\text{H}_2\text{O}$), anhydrous sodium sulfite P.A. (Na_2SO_3), sodium hydroxide P.A. (NaOH), hydrochloric acid (HCl), phthalic anhydride P.A. and glycerin P.A. were purchased from Vetec (Rio de Janeiro, Brasil). All chemicals were used as received. The deionized water (H_2O) was produced at LaBioS/IMA/UFRJ. Castor oil and crude oil were kindly donated by Petrobras. The crude oil sample tar type presented viscosity equal to (7006 ± 10) mPas, water content of $(11.5 \pm 0.4)\%$ v/v; density of 0.97 ± 0.01 g/cm⁻³ and °API (at 60°F) equal to (13.40 ± 0.01) .

Maghemite Synthesis: The maghemite was synthesized by a coprecipitation method using alkaline solution as described in the literature.^{6,15,18-24} The procedure involved preparing an alkaline solution containing 0.14 mol L⁻¹ of iron chloride (FeCl_3) in 200 mL of deionized water. The reaction mixture was left under magnetic stirring at room temperature and N₂ gas flow.

After iron chloride dilution was completed, 0.10 mol L⁻¹ of sodium sulfite (Na_2SO_3) and 0.64 mol L⁻¹ of hydrochloric acid (HCl) were added, keeping the initial conditions for stirring and temperature and limiting the amount of air in the medium. As expected, the reaction medium color changed when the solution was poured into the 0.1 mol L⁻¹ sodium hydroxide, under strong stirring (100 rpm).²⁴ At that moment, maghemite particles formed, which were then separated using a magnet (Nd – 2000 Gauss).

Alkyd Resin Synthesis and Preparation of Magnetizable Composites: The alkyd resin was synthesized following the generation of cross-linked polyesters in our research group.⁶ Three kinds of

Table I. Alkyd Resins/Composites Matrix Composition

Reactants	Resins		
	R1	R2	R3
Phthalic anhydride (g)	59	58	56
Castor oil (g)	4	7	10
Glycerin (g)	37	35	34

alkyd resins were synthesized, with distinct amounts of castor oil: 4, 7, and 10 g, which is equal to 4, 7, and 10% w/w. The amounts used in these syntheses are shown in Table I.

The procedure used to obtain the alkyd resins was performed inside a 500 mL reactor. Initially, phthalic anhydride, glycerin and castor oil were added to the reactor. The reactor was locked and a reflux condenser was then connected to it. This system was held at 240°C for 20 minutes, using a silicon bath. After that, the temperature was slowly increased, using a rate of 10°C/min, to dissolve the phthalic anhydride. After this step, the system was put under a vacuum. The reaction was stopped when the viscosity achieved a value that meant that it was impossible for the magnet to continue stirring. The composites were prepared using the same procedure, via *in situ* polymerization. The composite fillers were previously mixed in the glycerin to make the dispersion inside the polymeric matrix easy. The fillers used were 5% w/w maghemite and 5% w/w coffee grounds. The materials obtained from these syntheses were named from C1 to C3. All synthesized materials were macerated to provide a kind of powder, which made easier their posterior use.

Materials Characterization

Fourier Transformed Infrared with Attenuated Total Reflectance (FTIR-ATR). The obtained materials were dried at 80°C in the furnace up to constant weight. After that, they were held in a desiccator. The FTIR-ATR spectra were obtained using the equipment iN10 from Nicolet at room temperature and atmosphere, with a resolution of 4 cm⁻¹ and 100 accumulated scans.

X-ray Diffraction (XRD). The analyses were performed at room temperature, using an X-ray diffractometer Miniflex from Rigaku, with a radiation source that presented a potential difference of 30 kV and electric current of 15 mA. The equipment target was a copper plate that produces CuK α radiation with a wavelength of 0.154 nm. The scan was carried out at 2 θ values from 10° to 80°, with a goniometer step of 0.05°/min. The crystallite size (Lc) was calculated using the Scherrer equation [eq. (1)]²⁵:

$$Lc = K\lambda / (\beta \cos\theta) \quad (1)$$

In this eq. (1), Lc is the crystallite size, λ is the wavelength, β is the half-width and θ is the angle. The crystalline degree (Xc) was estimated using eq. (2), the Ruland method²⁶:

$$Xc = (Ac^*100) / (Ac + Aa) \quad (2)$$

Where, Ac is the crystalline area and Aa is the amorphous area.

Degree of Cross-Linking. After the samples were weighed, they were put inside the Soxhlet extractor in a filter paper package.

To perform the solvent extraction process, an equivolumetric mixture of toluene, heptane and cyclohexane at 250°C was used. Then, the samples were dried and weighed again to determine the weight lost and, consequently, the degree of cross-linking.²⁷

Apparent Density. These tests were carried out by measuring the weight of the materials inside a 10 mL graduated cylinder. After that, the volumes were determined and the apparent density values were calculated. Every measure was performed in triplicate.

Thermogravimetric Analyses. These analyses were carried out using the STA 6000 equipment from Perkin Elmer. The conditions used were a heating ramp method from 30°C to 700°C with an isotherm of 3 min at 700°C, a heating rate of 10°C min⁻¹ and a nitrogen inert atmosphere in platinum pans.

Magnetic Force. The magnetic force was established using a homemade apparatus composed of a lab balance, a removable support connected to an electromagnet, a sampler, a voltmeter, and an amperemeter.²⁴ The samples were submitted to a magnetic field, produced by an electromagnet, 5.5 ± 0.2 mm from the samples. The magnetic field intensity, measured in Gauss, was increased by applying an electric current from 0.00 to 0.9 A using a step of 0.05 A. The sample weight was measured in each step and the weight variation was determined. The magnetic force can be calculated using the following equation:

$$MF = \Delta w \cdot g \quad (3)$$

where the MF is the magnetic force, Δw is the weight variation in presence of magnetic field and g is gravitational acceleration.

Scanning Electron Microscopy (SEM) and Energy-Dispersive X-ray Spectroscopy (EDX). The analyses were performed using a scanning electronic microscope (SEM) from EI Quanta, Model 400 FEG, under vacuum with a secondary electron detector from Everhart-Thornley – ETD. The use of energy-dispersive X ray spectroscopy (EDX) associated with SEM was selected to determine the iron oxide agglomerates on the sample surface.

Water Absorption. The water absorption tests were carried out based on the ASTM F 726-81 standard. In these analyses, initially, the materials were dried up to constant weight, being kept in a desiccator. In the second step, they were immersed in water for 20 minutes. After that, they were weighed using an analytical balance. The change in weight is the amount of water absorbed in the material.

Crude Oil Magnetic Removal. These tests were performed at room temperature using synthetic brine, prepared using 50,000 ppm of sodium chloride and 5000 ppm calcium chloride. The crude oil used presented high visual viscosity, like a syrup, which makes crude oil removal from the water easy. In this kind of test, a 100 mL beaker containing 90 mL of brine was used, into which 0.5 g of crude oil was spilt. After that, a known weight of absorber composites was added onto the crude oil spot. The beaker was left for 5 min for the composites to interact with crude oil and form a semi-solid paste that could be removed using a magneto. The crude oil amount (Or) removed from the water was determined by gravimetry using the following equation:

$$Or = (w_2 - w_3) / w_1 \quad (4)$$

where w_1 is the used composite weight, w_2 is the total weight (beaker with water and crude oil), and w_3 is the system weight after removal (beaker with water and residual crude oil). This method allows the ratio between the removed crude oil and the composite, both in grams (g/g), to be calculated. The data obtained from this method were used to plot the absorption isotherm, which makes the data interpretation easier.

RESULTS AND DISCUSSION

Fourier Transform Infrared with Attenuated Total Reflectance (FTIR-ATR)

Figure 1 shows the main materials spectra from this work.

In the ground coffee spectrum shown in Figure 1(a), it is possible to see a band around 3500 cm⁻¹ related to stretching of bond O-H. This band is wide because of the hydrogen bonds formed in this kind of group. Moreover, this band is very intense because there are many compounds with this kind of bond in the ground coffee.²⁸ The maghemite spectrum can be observed in Figure 1(b). There are some important characteristic bands of this type of compound, such as the band around 3420 cm⁻¹, which is associated with stretching of the O-H group because of the presence of FeOH. There is a characteristic band related to the presence of structural water at 1632 cm⁻¹, while the characteristic band at 644 cm⁻¹ is associated with stretching of the Fe-O bond. These characteristic bands indicate successful maghemite synthesis.^{15,17-19} The alkyd resin spectrum is shown in Figure 1(c), where the characteristic band at 1750 cm⁻¹ corresponds to stretching of C=O bond. The C(C=O) groups vibration can be observed at 1270 cm⁻¹. The stretching of esters and ethers can be seen at 1115 and 1036 cm⁻¹, respectively. The (C=O)O groups vibration appears at 1045 cm⁻¹. Also, a decrease in the intensity of the hydroxyl group characteristic band intensity can be seen at around 3500 cm⁻¹.^{6,29} All synthesized alkyd resins were also tested and present similar FTIR spectra. The composite spectrum presented the same characteristic bands as those seen for alkyd resin, which indicates that the fillers did not change the chemical nature of the polymeric matrix.³ The other two composites were tested too and they presented the identical profile.

X-ray Diffraction (XRD)

Figure 2 presents the sample diffractograms.

Figure 2(a,b) present the diffractograms of ground coffee and alkyd resin, respectively. In both diffractograms an amorphous halo can be seen, which indicates that both materials are predominantly amorphous. In Figure 2(c), the maghemite diffractogram is presented, which exhibits the following diffraction peaks, in 2θ values: 30.5°, 35.8°, 43.1°, 53.9°, 57.5°, and 62.9°. These peaks correspond to the (220), (311), (400), (422), (511), and (440) crystalline planes in an orthorhombic cell of the cubic spinel structure, respectively.³⁰ This kind of crystalline structure is characteristic of γ -Fe₂O₃-type paramagnetic particles.²⁴ The diffractogram for the composite containing maghemite and ground coffee shows maghemite peaks and the amorphous halo as well. The crystallinity value and the crystallite sizes were calculated for maghemite and composites

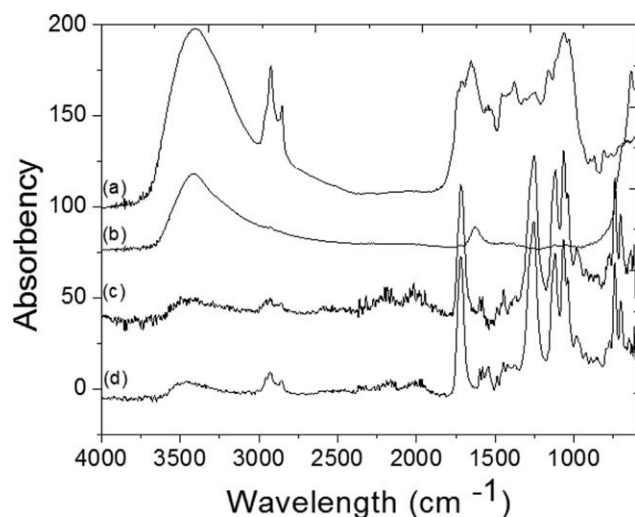


Figure 1. FTIR spectra of (a) ground coffee, (b) maghemite, (c) alkyd resin, and (d) composite C3.

containing 4%, 7%, and 10% of castor oil. The synthesized maghemite presented a crystallinity equal to $(67.1 \pm 2.1)\%$, which is a small value when compared with those in the literature.⁶ This crystallinity value indicates that the maghemite was contaminated by waste salts from the synthesis process. The composites presented similar crystallinity values with an average value of $(26.9 \pm 4.7)\%$. The crystallite sizes (L_c) were calculated from the peak at 2θ that was equal to 35.8° , which represents the (311) crystalline plane for maghemite and composites containing different amounts of castor oil. The average maghemite crystallite size (L_c) was (7.7 ± 0.9) nm, while the composites from C1 to C3 had average crystallite sizes of (6.4 ± 0.9) nm, (7.6 ± 1.1) nm and (8.8 ± 0.3) nm, respectively. These values are statistically the same, which proves that the nanoparticles did not suffer any changes during the matrix mixture process, keeping their properties.^{19,20}

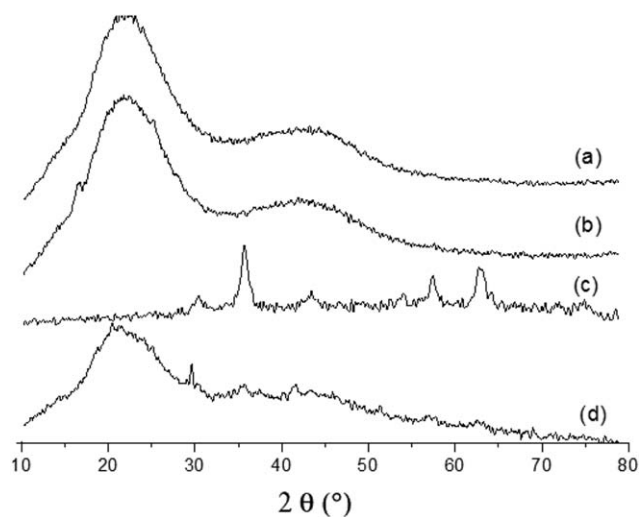


Figure 2. Diffractogram of (a) ground coffee, (b) alkyd resin, (c) maghemite, and (d) composite C3.

Table II. CLD and Apparent Density for Resins and Composites

Sample	CLD (%)	Apparent density (g/cm^3)
R1	86.1 ± 1.7	0.52 ± 0.01
R2	92.5 ± 1.1	0.55 ± 0.05
R3	95.0 ± 0.5	0.49 ± 0.02
C1	86.8 ± 1.6	0.46 ± 0.01
C2	93.2 ± 2.2	0.43 ± 0.05
C3	97.8 ± 1.9	0.40 ± 0.07

Magnetic Force

The magnetic force tests were performed using the methodology established by our research group²⁰; the results for maghemite and the composites from C1 to C3 were (591 ± 55) , (38 ± 3) , (32 ± 1) , and (41 ± 1) mN/g, respectively. As expected, the magnetic force of pure maghemite was stronger than that of the composites. However, the magnetic force achieved in the composites is sufficient for use in the removal of crude oil from the water surface, as can be seen in other works by our research group.^{2,4,6}

Cross-Linked Degree and Apparent Density

The cross-linked degree (CLD) and apparent density enabled verification of the effect of the insertion of fillers in the studied systems. These results are presented in Table II.

Table II presents the values of CLD and apparent viscosity. About CLD, it can be noticed the amount of castor oil is more influent than the fillers presence, the smallest CLD was obtained to both, resin and composite, with 4% w/w of castor oil. There is no significant variation in the CLD value in presence of fillers, for the same composition. Another fact, the CLD value seems increasing with the increment of castor oil amount. This result is strongly positive because the crude oil recovery and reuse of the absorber are directly related to the CLD. Higher values of this property promote chemical stability, which makes the absorber loss during the process smaller. With regard to the apparent density, the results are statistically equal when the

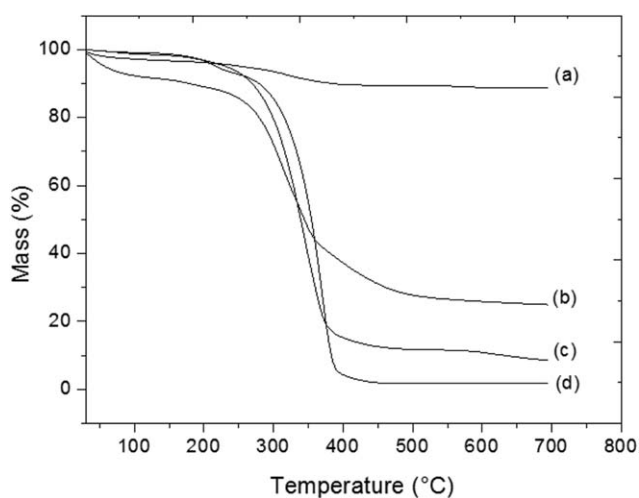


Figure 3. TGA of (a) maghemite, (b) coffee ground, (c) composite C3, and (d) alkyd resin.

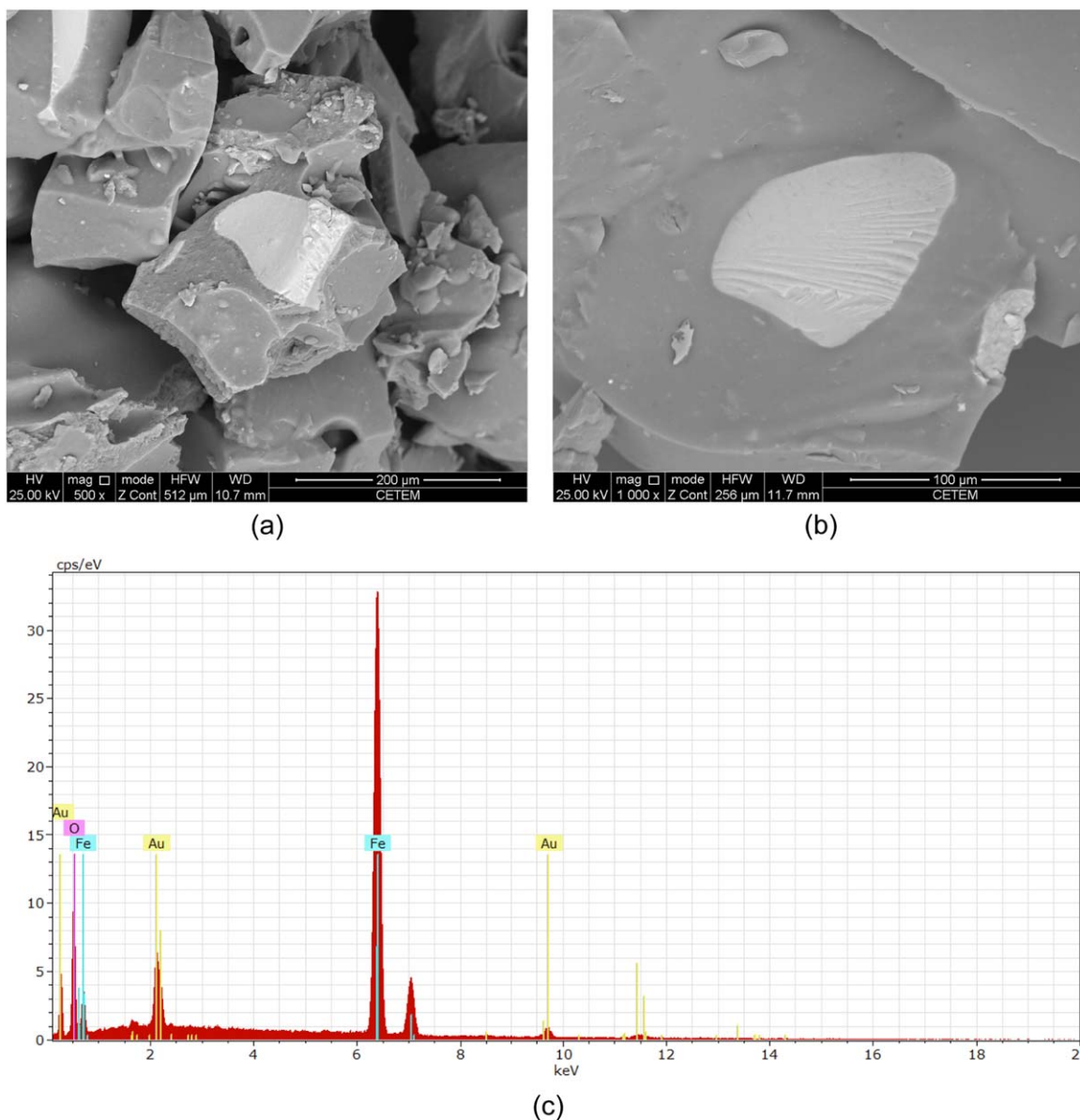


Figure 4. Composite containing 20% castor oil/glycerin SEM at (a) 500 \times , (b) 1000 \times , and (c) EDX spectrum. [Color figure can be viewed in the online issue, which is available at wileyonlinelibrary.com.]

resins are compared their selves. The same behavior is observed in composites. However, the results are closely distinct when these two groups are compared. These results show effect of the coffee ground as a reducer of the density in the composites, once the iron oxide has an apparent density around 5 g/cm³. That property is fundamental to guaranteeing the floatation of materials during the removal process on water surfaces.

Thermogravimetric Analyses

Figure 3 shows the TGA of some of the main prepared composites. Maghemite presents a typical inorganic material mass loss profile, showing the highest thermal stability, followed by the composite containing maghemite and coffee grounds, then pure resin, and the smallest thermal stability being presented by pure coffee grounds. The maghemite presented two main mass loss regions, in which the maximum mass loss rates occurred at

(100 \pm 2) $^{\circ}$ C and (567 \pm 6) $^{\circ}$ C for the elimination of water that was physically and chemically absorbed in the material, respectively.³¹ As expected, the coffee ground showed weight diminishing related to water and light organic chemicals at low temperatures, starting at (211 \pm 3) $^{\circ}$ C.

The nanocomposite shown in Figure 3(c) presents a degradation profile that is very similar to that of pure resin. The resin and composites TGA curves presented three mass loss processes in which the rates are (90 \pm 12) $^{\circ}$ C, (210 \pm 17) $^{\circ}$ C and (358 \pm 21) $^{\circ}$ C, respectively. The first process is related to light organic chemicals from the polymerization process. The second weight loss process is associated with the elimination of lighter molar mass compounds and the third one refers to the resin thermo-oxidative degradation.³² These results, together with the CLD, make it clear that the prepared composites can be heated during

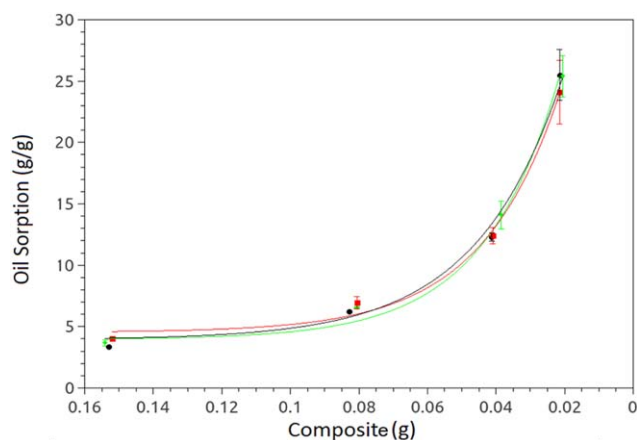


Figure 5. Crude oil absorption isotherm from the composites C1 (●), C2 (■) e C3 (▲). [Color figure can be viewed in the online issue, which is available at wileyonlinelibrary.com.]

the crude oil recovery process in the presence of organic solvents without thermal or chemical degradation.

Water Absorption Capability

The average value of absorbed water amount to resins was (1.2 ± 0.2) g/g, while to composites was (0.8 ± 0.2) g/g. It can be seen that the distinct amounts of castor oil used in the resin, or composites, composition did not promote any effect in the amount of water absorbed by these materials. Besides, the inorganic nanoparticles containing a small quantity of absorbed water as seen in the TGA result. However in this test, the inorganic nanoparticles presence, in the composite, did not produce any changes in the absorbed water amount.

Scanning Electron Microscopy (SEM) and Energy-Dispersive X-ray Spectroscopy (EDX)

The morphology of the composite containing coffee grounds and maghemite nanoparticles is shown in Figure 4(a,b). In this image, it is possible to see that grain fractures are irregular and smooth, which are typical characteristics of tough and brittle materials. Also, the grains presented a smooth surface and irregular shape, which suggests that the crude oil removal mainly occurred via chemical interactions between the materials, as the particles did not present visible porosity. This result corroborates the previous study performed. In this study it was showed that the removal capability is higher when resins more chemically similar to crude oil are used.² The particle morphology, which was tough and brittle, supported material reuse because of the high mechanical strength.

Figure 4(b) shows a lighter region, marked with number 2, which may be related to the agglomerated maghemite nanoparticles. This was confirmed by the EDX analyses, as shown in

Figure 4(c), where it is possible to observe peaks from some chemical elements, with iron being the most intense. The presence of regions with agglomerated iron indicates that the *in situ* addition methodology was not efficient enough to disperse the nanoparticles in the matrix bulk; on the other hand, the composite magnetic force (38 ± 3) mN/g was strong enough to be used in the crude oil removal process, even though the composite magnetic force was around 10 times less than that of pure maghemite (591 ± 55) mN/g.

Crude Oil Magnetic Removal

These tests allow the crude oil absorption isotherm to be built, as shown in Figure 5.

Data used to plot in Figure 5 were analyzed by the following model, shown in the following equation:

$$RO = RO_0 + A \cdot e^{(-R/\rho)} \quad (5)$$

where RO is the crude oil removal capability, RO_0 corresponds to the lower amount of crude oil removed, A represents the function amplitude, R is the amount of resin used in each crude oil removal process and ρ corresponds to the system decay constant. The results obtained from this model are shown in Table III.

From analyzing Figure 5 and Table II, it is possible to see that every parameter is statistically equal, which enabled the conclusion that the amount of castor oil used, 4%, 7%, and 10%, did not alter the crude oil removal capability of the composites. These results show that each gram of composite is able to remove around (25 ± 1) g of crude oil, which indicates that the composites are chemically similar to crude oil. In addition, the crude oil removal capability values obtained for these materials are the highest obtained in this research group,^{2-4,14} and were associated with lower water absorption, allowing us to confirm that these materials are very promising for application in oil spill accident scenarios with the subsequent crude oil removal and recovery process.

CONCLUSION

The bulk polymerization was able to produce thermoset crude oil absorbers, generating high CLD polymers. The *in situ* filler addition methodology used to obtain composites with two fillers, an organic and an inorganic, was very successful. The fillers were inserted in the matrix bulk and did not change the physical and chemical properties of either phase. The composites produced showed high crude oil chemical affinity and low chemical affinity with the water. This behavior shows that the composites are more oleophilic, making these composites useful for the crude oil removal process. Therefore, the use of coffee grounds can be considered a sustainable measure in the production of polymers. The reuse of these materials, as well as producing high volumes of vegetable waste, also contributes to the

Table III. Exponential Model Parameters and its Respective Correlations

Sample	A	ρ	RO_0	R^2
C1	$(5.7 \pm 1.1) \times 10^1$	$(2.2 \pm 0.4) \times 10^2$	$(4.0 \pm 1.1) \times 10^0$	0.9949
C2	$(4.9 \pm 1.0) \times 10^1$	$(2.3 \pm 0.5) \times 10^2$	$(4.5 \pm 1.1) \times 10^0$	0.9937
C3	$(4.8 \pm 0.5) \times 10^1$	$(2.5 \pm 0.3) \times 10^2$	$(3.9 \pm 0.8) \times 10^0$	0.9976

final properties of the magnetizable composites, mainly in the apparent density decrease, which increases the floatability, and thus making the removal of oil from water surfaces easy. The crude oil magnetic removal tests showed that one gram of the composite containing 5% coffee grounds and 5% maghemite is able to remove (25.06 ± 1.18) g of crude oil. Evaluating all of the synthesized composites, it is possible to conclude that the castor oil amount did not cause any change in the composite properties, including the crude oil removal capability. Considering this last statement, it is suggested that the use of the magnetizable composite containing 10% castor oil is related to the amount of glycerin because, in this case, a larger amount of castor oil, a toxic waste, is taken away from the environment. It can therefore be considered another sustainable measure.

ACKNOWLEDGMENTS

The authors thank Conselho Nacional de Desenvolvimento Científico e Tecnológico (CNPq-474940/2012-8 and 550030/2013-1), Coordenação de Aperfeiçoamento de Pessoal de Nível Superior (CAPES and CAPES-MES Cuba # 154/12), Financiadora de Estudos e Projetos (FINEP PRESAL Ref.1889/10), LABEST/PEC/COPPE/UFRJ laboratory by SEM, ASCONTEC ABRASIVOS by alumina powder and Reduc/Petrobras by paraffin and Fundação Carlos Chagas Filho de Amparo à Pesquisa do Estado do Rio de Janeiro (FAPERJ E-26/201.498/2014) for the financial support and scholarships. The authors also thank the LABIOS/IMA/UFRJ for volunteer Post-Doc position to Oliveira, G. E.

AUTHOR CONTRIBUTIONS

F. D. Marques prepared all resins and composites studied in this work. She has performed the materials characterization and crude oil removal test. She wrote the first draft of this work in Portuguese, with the previous data interpretation. She approved the submitted final version. G. E. Oliveira supported the analysis plan and data interpretation, mainly related to FTIR-ATR, TGA, and crude oil magnetic removal results. She reviewed this work some times and translated it to English. She approved the submitted final version. F. G. Souza Jr. planned the analysis, provided conditions to performed the analysis plan and support data interpretation, mainly related to DRX, SEM, EDX, water absorption capability, magnetic force, degree of cross-linked and crude oil magnetic removal results. He reviewed this work some times and approved the submitted final version.

REFERENCES

1. Kingston, P. F. *Spill Sci. Technol. Bull.* **2002**, *7*, 53.
2. Grance, E. G. O.; Souza, F. G., Jr.; Varela, A.; Pereira, E. D.; Oliveira, G. E.; Rodrigues, C. H. M. *J. Appl. Polym. Sci.* **2012**.
3. Ferreira, L. P.; Moreira, A. N.; Delazare, T.; Oliveira, G. E.; Souza, F. G., Jr. *Macromol. Symp.* **2012**, *319*, 210.
4. Varela, A.; Oliveira, G.; Souza, F. G.; Rodrigues, C. H. M.; Costa, M. A. S. *Polym. Eng. Sci.* **2013**, *53*, 44.
5. Farag, R. K.; El-Saeed, S. M. *J. Appl. Polym. Sci.* **2008**, *109*, 3704.
6. Oliveira, G. E.; Souza, F. G., Jr.; Lopes, M. C. in *Natural Polymers, Biopolymers, Biomaterials, and their Composites, Blends, and IPNs*, 1st ed.; CRC Press: Toronto, **2012**; Chapter 22, p 370.
7. Ayman, A. M.; El-Hamouly, S. H.; Al Sabagh, A. M.; Gabr, M. M. *J. Appl. Polym. Sci.* **2007**, *104*, 871.
8. Wyatt, V.; Yadav, T. M. *J. Appl. Polym. Sci.* **2013**, *130*, 70.
9. Ferreira, T. Universidade Federal Do Rio Grande Do Norte **2009**.
10. Guzel, S.; Erol, O.; Ibrahim Unal, H. *J. Appl. Polym. Sci.* **2012**, *124*, 4935.
11. Lopes, M. C.; Souza, F. G., Jr.; Oliveira, G. E. *Polímeros* **2010**, *20*, 359.
12. Souza, F. G., Jr.; Marins, J. A.; Rodrigues, C. H. M.; Pinto, J. C. *Macromol. Mater. Eng.* **2010**, *295*, 942.
13. Bal, A.; Acar, I.; Güçlü, G. *J. Appl. Polym. Sci.* **2012**, *125*, E85.
14. Elias, E.; Costa, R. M. D.; Marques, F. D.; Oliveira, G. E.; Guo, Q.; Thomas, S.; Souza Jr., F. G. *J. Appl. Polym. Sci.* **2014**, *132*, 41732.
15. Souza, F. D. E.; Marins, J.; Pinto, J.; Oliveira, G. D. E.; Rodrigues, C.; Lima, L. *J. Mater. Sci.* **2010**, *45*, 5012.
16. Kondamudi, N.; Mohapatra, S. K.; Misra, M. *J. Agric. Food Chem.* **2008**, *56*, 11757.
17. Issa, B.; Obaidat, I. M.; Albiss, B. A.; Haik, Y. *Int. J. Mol. Sci.* **2013**, *14*, 21266.
18. Pereira, E. D.; Souza, F. G.; Santana, C. I.; Soares, D. Q.; Lemos, A. S.; Menezes, L. R. *Polym. Eng. Sci.* **2013**, *53*, 2308.
19. Pereira, E. D.; Souza, F. G., Jr.; Pinto, J. C. C. S.; Cerruti, R.; Santana, C. *Macromol. Symp.* **2014**, *343*, 18.
20. Costa, R. C. D. A.; Souza, F. G., Jr. *Polímeros* **2014**, *24*, 243.
21. Souza, F. G., Jr.; Ferreira, A. C.; Varela, A.; Oliveira, G. E.; Machado, F.; Pereira, E. D.; Fernandes, E.; Pinto, J. C.; Nele, M. *Polym. Test.* **2013**, *32*, 1466.
22. Ferreira, G.; Segura, T.; Souza, F. G., Jr.; Umpierre, A. P.; Machado, F. *Eur. Polym. J.* **2012**, *48*, 2050.
23. Neves, J. S.; Souza, F. G., Jr.; Suarez, P. A. Z.; Umpierre, A. P.; Machado, F. *Macromol. Mater. Eng.* **2011**, *296*, 1107.
24. Péres, E. U. X.; Souza, F. G., Jr.; Silva, F. M.; Chaker, J. A.; Suarez, P. A. Z. *Ind. Crops Prod.* **2014**, *59*, 260.
25. Scherrer, P. *Nachr. Ges. Wiss. Math.-Phys. Kl.* **1918**, *98* (n.d.).
26. Ruland, W. *Acta Crystallogr.* **1961**, *14*, 1180.
27. O'connor, D.; Blum, F. D. *J. Appl. Polym. Sci.* **1987**, *33*, 1933.
28. Wang, N.; Lim, L. T. *J. Agric. Food Chem.* **2012**, *60*, 5446.
29. Dutra, R. C. L.; Takahashi, M. F. K.; Diniz, M. F. *Polímeros* **2012**, *12*, 273.
30. Oliveira, G. E.; Clarindo, J. E. S.; Santo, K. S. E.; Souza, F. G., Jr. *Mater. Res.* **2013**,
31. Xie, Y.; Sougrat, R.; Nunes, S. P. *J. Appl. Polym. Sci.* **2015**, *132*, 41368.
32. Gogoi, P.; Saikia, B. J.; Dolui, S. K. *J. Appl. Polym. Sci.* **2015**, *132*, 41490.